Aquaporin 3 (Gill Blood Group) (AQP3): Machine Learning Discoveries of 2nd Order Synergy in Meningiomas

Shriprakash Sinha *

Posted Date: 26 May 2025

doi: 10.20944/preprints202505.1982.v1

Keywords: AQP3; meningioma; sensitivity analysis; machine learning

 doi:10.20944/preprints202505.1982.v1

Article

Aquaporin 3 (Gill Blood Group) (AQP3): Machine Learning Discoveries of 2^{nd} Order Synergy in Meningiomas

Shriprakash Sinha

Independent Researcher, 104-Madhurisha Heights Phase 1, Risali, Bhilai-490006, India; sinha.shriprakash@yandex.com

Abstract: Background: AQP3 belongs to the family of aquaporins (or water channels), which are membrane proteins from a larger family of major intrinsic proteins (MIP) that form pores in the membrane of biological cells. Genetic defects in aquaporins have been associated with several human diseases. Meningiomas are the most common intracranial primary neoplasm in adults. [1] analyzed 160 tumors from all 3 World Health Organization (WHO) grades (I through III) using clinical, gene expression, and sequencing data and using unsupervised clustering analysis identified 3 molecular types (A, B, and C) that reliably predicted recurrence. Further, these groups did not directly correlate with the WHO grading system, which classifies more than half of the tumors in the most aggressive molecular type as benign. **Issue**: Increasing evidence point to the fact that meningioma classification and grading, that is based on histopathology does not always accurately predict tumor aggressiveness and recurrence behaviour and knowledge of the underlying biology of the treatment resistant meningiomas and the impact of genetic alterations in these tumors, is lacking. At the current stage more genomic studies are required to unravel the role of other genes and their interations with other genetic factors. **Resolution**: In a recently published work Sinha [2], a frame work of a search engine was developed which can rank combinations of factors (genes/proteins) in a signaling pathway. Adapting this search engine to the Meningioma dataset, i present here 2^{nd} order combinations of AQP3, some of which have been known to exist via wet lab experiments, but many are yet to be tested. The reveals combinations might help oncologists/biologists test possible hypotheses that might be the causing factors in meningioma. Further, in my limited grasp, if proven true, the combinations revealed by the search engine might pave way for development of gene based therapies aimed at resolving pathological issues related to meningiomas.

Keywords: AQP3; meningioma; sensitivity analysis;machine learning

1. Introduction

1.1. Meningioma

Meningiomas are the most common intracranial primary neoplasm in adults. They arise from the arachnoid cap cells. These arachnoid cap cells are specialized cells that make up the arachnoid mater (one of the three protective memberanes covering the brain and spinal cord). The arachnoid mater is one of the three meninges. The other two that constitute the meninges are dura mater and pia mater.

1.1.1. World Health Organization (WHO) Classification

The meningiomas are classified into three grades by WHO under the Central Nervous System tumours, namely, Grade I (benign), Grade II (atypical) and Grade III (anaplastic/malignant), based on histopathology or subtype (Louis et al. [3]). As of 2021, there exists 12 histopathological meningioma subtypes according to a mini-review by [4]. They are meningothelial, fibrous, transitional, psammomatous, angiomatous, microcystic, secretory, lymphoplasmacyte-rich, atypical, chordoid, clear cell and anaplastic (malignant) meningioma.

 doi:10.20944/preprints202505.1982.v1

1.1.2. Historical perspective

Czarnetzki et al. [5] investigated a skull that was excavated at Steinheim/Murr (Baden-Wurttemberg, Germany) and consisted of a well preserved plagiocephalic cranium, with most of the facial skeleton intact. Their results of stratigraphical dating suggested the fossil specimen of Homo steinheimensis, was about 3,65,000 years old. In the fossile, they found that several features of the inner cranial table were consistent with a diagnosis of meningioma. As documented in [6], in 1614, Felix Plater, Professor of Medicine, issued a case report from the University of Basel on Caspar Bonecurtius, a noble knight stating -

> began to lose his mind gradually over a two year period, to such an extent that finally he was completely stupefied and did nothing rationally. He had no desire for food and ate only when forcibly fed. ... Finally after matters had gone on thus for six months, he died.
>
> Further, the autopsy report of Plater stated the following -
>
> a round fleshy tumor, like an acorn. It was hard and full of holes and was as large as a medium-sized apple. It was covered with its own membrane and was entwined with veins. However, it was free of all connections with the matter of the brain, so much so that when it was removed by hand, it left behind a remarkable cavity.

This was the first case in the history that documented a patient with a lesion that was most compatible with a meningioma.

Next, in a contribution by Italian scientists, Paterniti [7] documents the first contribution of Andrea Vacca' Berlinghieri in 1813 in a manuscript Trattato di Chirurgia Pratica, which was never published. Its discovery was made accidentally by David Giordano, who referred in detail in an article on surgeon of Pisa in La chirurgia di Andrea Vacca' Berlinghieri. Riv Storia Sci MedNat. 1927: XVIII (3-4): 75-106. The unpublished manuscript of 488 pages describes that Vacca Berlinhieri proposed and performed a most bold radical operation. After a craniectomy with five or six burr holes on the outskirts of the fungus, the tumor was removed together the dura mater from which it originated, tying the cut vessels.

In 1847, Zanobi Pecchioli, Professor of Clinical Surgery and Operative Medicine at Modena and then at Siena University, published an account of surgeries performed during 16 years, from 1832 to 1847 (16 of the 1524 reported operations involved trephining of the skull). In one of these interventions, he carried out on July 29 1835, in Siena, for the resection of a meningioma, a defined fungus of the duramater. The case was not referred in the literature by Pecchioli but was described by in Pecchioli [8]. Finally, [9] coined the modern term of "meningioma".

1.1.3. Pathophysiology

Meningiomas arise from arachnoidal cap cells, most of which are near the vicinity of the venous sinuses, and this is the site of greatest prevalence for meningioma formation. The dural venous sinuses (also called dural/cerebral/cranial sinuses) are venous sinuses (channels) found between the periosteal and meningeal layers of dura mater in the brain. They receive blood from the cerebral veins, and cerebrospinal fluid (CSF) from the subarachnoid space via arachnoid granulations. They mainly empty into the internal jugular vein. Cranial venous sinuses communicate with veins outside the skull through emissary veins. These communications help to keep the pressure of blood in the sinuses constant. (contributors [10], Pamir et al. [11])

A schematic diagram for different pathways in different meningiomas has been provided in Figure 1.

 doi:10.20944/preprints202505.1982.v1

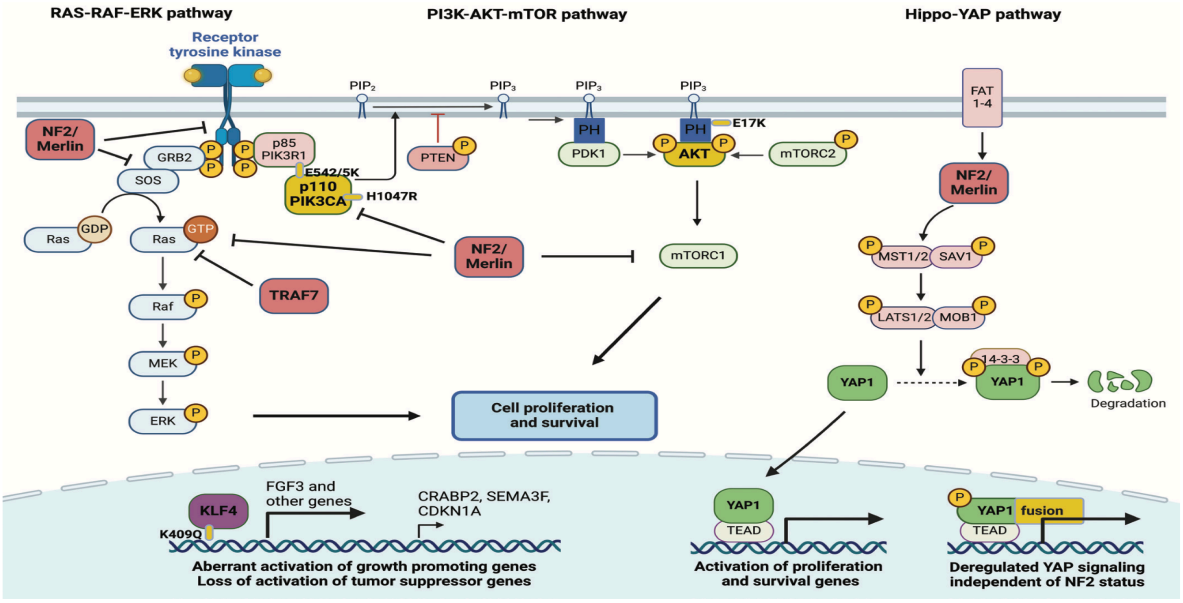

Figure 1. A schematic diagram of different pathways in different meningiomas, as provided by [12] under CC-BY Attribution 4.0 International license (https://creativecommons.org/licenses/by/4.0/)

1.2. Ion Channels

Ion channels, as the name suggests, as we deconstruct the terminology, in a lay man's term means, a channel or a passage that helps pass the ions. When we talk of passage, then the flow of the ions has to happen through something permeable, a wall, a barrier, an obstruction, etc. Also, the channel should open and close with some purpose and there has to be some definite aim, for which the channel behind which the passage will work. For other conditions, the channel has to remain closed. Investigating these conditions, will help in understanding the ambinence of the channel itself. Another aspect of particular importance is the fact regarding the kind of ions that will pass through the passage and why such ions need to pass through such a channel. Along with the study of these channels, comes the study of the varied structure of these channels which help the passage of these ions. All these issues gives rise to the field of simulation and modeling of these channels also.

Broadly speaking, ion channel is one of the two classes of an ionophoric proteins, that will let the ions pass downhill along with the electrochemical gradient in the channel without the input of any metabolic activity; the other being ion transporters. Ionophoric proteins are structures that reversibly binds with ions. Ion transporters are proteins that will carry the ions along with them through a permeable wall or barrier or an obstruction against a concentration gradient. This passage of the ions requires openning and closing mechanism in the channel and in electrophysiology, *gating* is the term used for such a mechanism. It is the process were the channel transforms from a conducting mode where ions flow to a non-conducting mode were ions do not pass through. The rate of closing and openning is referred to as *kinetics of gating*.

There are two major kinds of ion channels namely, (a) Voltage gated ion channel and (b) Ligand gated ion channel. The former operates via the difference in barrier or membrane voltage potential while the latter works via the binding of ligand to the channel. Also, there are different kinds of ions that go through the membrane. These include chloride, potassium, sodium, calcium and proton, to name a few. Depending on the kind of ions, certain functionalities are characteristics of a respective ion channel under study. But before I delve deeper into the specific area of interest, it is important to ask, what is the purpose of such a channel and why this gating process in helpful? The answer to this question will also address the ambience in which the channel is working or not working and thus build the context for the above posed question.

 doi:10.20944/preprints202505.1982.v1

1.3. The Discovery of Aquaporins and the 2003 Nobel Committee's Decisions

Aquaporins, also called water channels, are ion channel proteins that mainly facilitate transport of water between cells. The cell membranes contain aquaporins through which water can flow more rapidly into and out of the cell than by diffusing through the phospholipid bilayer.

The aquaporins (AQPs) are a family of small membrane-spanning proteins (monomer size approximately 30 kDa) that are expressed at plasma membranes in many cells types involved in fluid transport. [13] provide a review on the molecular structure and function of mammalian aquaporins. They suggest that aquaporins appear to assemble in membranes as homotetramers in which each monomer, consisting of six membrane-spanning alpha-helical domains with cytoplasmically oriented amino and carboxy termini, contains a distinct water pore. Their medium-resolution structural analysis by electron cryocrystallography indicated that the six tilted helical segments form a barrel surrounding a central pore-like region that contains additional protein density. Further, they observe that several of the mammalian aquaporins (e.g., AQP-1/2/4/5) appear to be highly selective for the passage of water, whereas others (recently termed aquaglyceroporins) also transport glycerol (e.g., AQP-3/8) and even larger solutes (AQP9). They state that results from knockout mice which implicate multiple physiological roles of aquaporins suggest that the aquaporins might be suitable targets for drug discovery by structure-based and/or high-throughput screening strategies.

In 1986, [14] examined the binding of [203Hg]-p-(chloromercuri)benzenesulfonate to the membrane proteins of human erythrocytes and erythrocyte ghosts, under conditions where binding to the bulk of membrane sulfhydryl groups was blocked by N-ethylmaleimide. They report that binding was complete within 90 min when approximately 40 nmol was bound per milligram of membrane protein. Their measurement by NMR technique revealed that this binding was correlated with the inhibition of water transport. Further, they observed maximal inhibition with the binding of approximately 10 nmol of p-(chloromercuri)benzenesulfonate/mg of membrane protein. Under these conditions, both band 3 and band 4.5 bound 1 mol of inhibitor/mol of protein. In contrast to previous experiments, their results indicated that band 4.5 proteins as well as band 3 had to be considered as playing a role in water transport.

In 1988, [15] identified a novel Mr 28,000 integral membrane protein ("28kDa") in human erythrocytes and found entirely associated with the Triton X-100 insoluble membrane skeletons. They reported that antibodies to 28kDa reacted strongly on immunoblots with 28kDa and a diffuse region of Mr 35,000-60,000 ("HMW-28kDa"). They further reported that selective proteolytic digestions of membranes demonstrated that HMW-28kDa has an extracellular domain, and both 28kDa and HMW-28kDa had intracellular domains. Their quantitative immunoblots indicated that each erythrocyte contained 120,000-160,000 copies of 28kDa. Their immunohistochemical staining of human kidney with anti-28kDa demonstrated prominent staining over the apical brush borders of proximal convoluted tubules. They purified a novel integral membrane protein from erythrocyte and kidney membranes and suggested that this new protein may play a role in linkage of the membrane skeleton to the lipid bilayer.

In 1992, [16] claimed that water rapidly crosses the plasma membrane of red blood cells (RBCs) and renal tubules through specialized channels and the molecular structure of these channels was unknown. Further, they state that CHIP28 protein was an abundant integral membrane protein in mammalian RBCs and renal proximal tubules and belonged to a family of membrane proteins with unknown functions. They observed that oocytes from Xenopus laevis microinjected with in vitro-transcribed CHIP28 RNA exhibited increased osmotic water permeability; this was reversibly inhibited by mercuric chloride, a known inhibitor of water channels. Thus they claimed that it is likely that CHIP28 is a functional unit of membrane water channels.

Following this, in 1993, [17], claimed that despite longstanding interest by nephrologists and physiologists, the molecular identities of membrane water channels remained elusive until recognition of CHIP, a 28-kDa channel-forming integral membrane protein from human red blood cells originally referred to as "CHIP28" (or aquaporin-1). They report that CHIP functioned as an osmotically driven,

 doi:10.20944/preprints202505.1982.v1

water-selective pore, observing the following - • expression of CHIP conferred Xenopus oocytes with markedly increased osmotic water permeability but did not allow transmembrane passage of ions or other small molecules and • reconstitution of highly purified CHIP into proteoliposomes permitted determination of the unit water permeability, i.e., 3.9 x 10(9) water molecules.channel subunit-1 x s-1. They state that although CHIP existed as a homotetramer in the native red blood cell membrane, site-directed mutagenesis studies suggested that each subunit contained an individually functional pore that may be reversibly occluded by mercurial inhibitors reacting with cysteine-189. Further, CHIP was a major component of both apical and basolateral membranes of water-permeable segments of the nephron, where it facilitates transcellular water flow during reabsorption of glomerular filtrate. Similar proteins from other mammalian tissues and plants were later shown to transport water, and the group was referred to as the "aquaporins". They state that recognition of CHIP provided molecular insight into the biological phenomenon of osmotic water movement, and it was hoped that pharmacological modulation of CHIP function might provide novel treatments of renal failure and other clinical problems.

An invited review of the history of the discovery of water channels proteins was published in September 2003 by [18], just one month before the Nobel Prize for Chemistry was awarded. Quoting a section of the abstract of [18], it states -

> In other words the child we first detected was recognized as having the predicted qualities only in 1992. In 1993 CHIP28 was renamed aquaporin 1. Looking in retrospect, asking the crucial question, when was the first water channel protein, aquaporin 1, discovered, a fair and clear cut answer would be: the first water channel protein, now called aquaporin 1, was identified or "seen" in situ in the human RBC membrane by Benga and coworkers in 1986. It was again "seen" when it was by chance purified by Agre and coworkers in 1988 and was again identified when its main feature, the water transport property was found by Agre and coworkers in 1992.

Table 1 of [18] shows the timeline of the discovery of the aquaporins and it has been heard that the Nobel Committee overlooked the contributions of the Benga group. Further, no mention of the results of Benga and coworkers appeared in the historical description of the discovery of aquaporins that joined the prize announcement. The link to the historical description by Nobel Committee can be found in Web Archive (https://web.archive.org/web/20081215025250/http://nobelprize.org/nobel_prizes/chemistry/laureates/2003/adv.html) and a copy of the information released by The Royal Swedish of Sciences in Advanced info. on the Nobel Prize in Chemistry, 8 Oct. 2003 (https://web.archive.org/web/20081203030151/http://nobelprize.org/nobel_prizes/chemistry/laureates/2003/chemadv03.pdf). In 2004, [19] acknowledges the work of Peter C. Agre, an American Society of Nephrology member and states that Agre's discovery of the first water channel has spurred a revolution in animal and plant physiology and in medicine. There is no mention of the work of Benga and coworkers in the starting abstract. Further, in a critical chronological analysis [20] voices his views on this topic while stating the following:

> Agre's group did include a reference to Benga's work in their Science paper; but this reference was only to a 1983 paper on protease resistance of "water channels" (which was relevant) and not the pertinent 1986 Biochemistry paper, or even the subsequent publications. The report of the recent exciting finding of possible involvement of aquaporins in epilepsy, published in 2005 in Proc Natl Acd Sci USA by a group including Agre failed to cite Benga and Morariu's novel and startling report in Nature in 1977.

Support for Dr. Gheorghe Benga and his coworkers has been documented at Link to contributions of Dr Gheorghe Benga (https://web.archive.org/web/20080129155507/http://www.ad-astra.ro/benga/index.php).

 doi:10.20944/preprints202505.1982.v1

1.4. Aquaporin 3 (AQP-3)

Ishibashi et al. [21] reported the cloning of a member of the water channel that also transports nonionic small molecules such as urea and glycerol and named this channel aquaporin 3 (AQP3) for its predominant water permeability. They observed that AQP3 had amino acid sequence identity with major intrinsic protein (MIP) family proteins including AQP-channel-forming integral membrane protein, AQP-collecting duct, MIP, AQP-gamma tonoplast intrinsic protein, nodulin 26, and glycerol facilitator (33-42%). Their measurement via ideomicroscopy, of the osmotic water permeability of Xenopus oocytes was 10-fold higher in oocytes injected with AQP3 transcript than with water-injected oocytes. Further, they observed that although to a smaller degree, AQP3 facilitated the transport of nonionic small solutes such as urea and glycerol, the previously cloned water channels were permeable only to water when expressed in Xenopus oocytes. They found that AQP3 mRNA was expressed abundantly in kidney medulla and colon, with it being exclusively immunolocalized at the basolateral membrane of collecting duct cells, in kidney. Thus they suggested that AQP3 might function as a water and urea exit mechanism in antidiuresis in collecting duct cells.

After screening a human kidney cDNA library with rat AQP3 probe and isolating a cDNA coding for human AQP3 protein, [22] determined the structure, tissue distribution, and chromosomal localization of the human AQP3 gene. They inferred that the amino acid sequence of human AQP3 was 91% identical to rat AQP3 and human AQP3 gene was mapped to 7q36.2-q36.3. Further, they found that human AQP3 mRNA was expressed in colon, kidney, liver, pancreas, lung, peripheral leukocytes, spleen, and prostate.

Ref. [23] isolated the human aquaporin 3 (AQP3) gene, and characterized its structural organization. They observed that the gene appeared to exist as a single copy in the human genome and comprised of six exons distributing over 7 kilobases, while enumerating the sizes of the exons and introns. Further, they identified the initiation site of transcription to locate 64 base pairs upstream of the first ATG codon. They also observed that the 5′-flanking region had a TATA box, two Sp1 sequences, and some consensus sequences including AP2 sites. With luciferase assay, they demonstrated that the 5′-flanking region had a promoter activity, which was up-regulated 4-fold by phorbol ester. Through their findings about the human AQP3, they thought that it will elucidate the molecular mechanism of transcriptional regulation of AQP3.

Ref. [24] determined the chromosome location of AQP3 and showed that in situ hybridization on metaphase chromosomes allowed the assignment of human AQP3 to chromosome 9p21–>p12.

Ref. [25] isolated the mouse AQP3 cDNA which encoded a 292-amino acid water/glycerol-transporting glycoprotein expressed in kidney, large airways, eye, urinary bladder, skin, and gastrointestinal tract. They analyzed the mouse AQP3 gene, and generated AQP3 null mice via targeted gene disruption. They observed that the fluid consumption in AQP3 null mice was more than 10-fold greater than that in wild-type litter mates, and urine osmolality (<275 milliosmol) was much lower than in wild-type mice (>1,200 milliosmol). After administration of 1-desamino-8-d-arginine-vasopressin administration or water deprivation, they found that the AQP3 null mice concentrated their urine partially to approximately 30% of that in wild-type mice, while osmotic water permeability of cortical collecting-duct basolateral membrane, was >3-fold reduced by AQP3 deletion. To test the hypothesis that the residual concentrating ability of AQP3 null mice was due to the inner medullary collecting-duct water channel AQP4, they generated AQP3/AQP4 double-knockout mice. This double-knockout mice had greater impairment of urinary-concentrating ability than did the AQP3 single-knockout mice. Their findings proved a form of nephrogenic diabetes insipidus produced by impaired water permeability in collecting-duct basolateral membrane. They concluded that basolateral plasma membrane aquaporins (AQP3) of kidney collecting-duct epithelial cells, might thus provide blood-accessible targets for drug discovery of aquaretic inhibitors.

By protein and molecular biology analysis, [26] found that the two unrelated probands who developed alloantibodies to the high frequency antigen GIL, were AQP3-deficient. They identified that this defect was caused by homozygous mutation affecting the 5′ donor splice site of intron 5 of the

 doi:10.20944/preprints202505.1982.v1

AQP3 gene, which led to skipping of exon 5 and generated a frameshift and premature stop codon. Their functional studies revealed the absence of facilitated glycerol transport across red cell membranes from the probands, but the water and urea transports were normal. Further, their expression studies showed that only cells transfected with AQP3 cDNA strongly reacted with anti-GIL antibodies. Thus their findings represented the first reported cases of AQP3 deficiency in humans and provided the molecular basis of a new blood group system, GIL, encoded by the AQP3 protein.

Ref. [27] used RNA sequencing (RNA-seq) to determine whole transcriptome profiles of twenty meningiomas with genomic alterations including NF2 inactivation, loss of chr1p, and missense mutations in TRAF7, AKT1 and KLF4. Their examination of TRAF7 tumors demonstrated that TRAF7 regulated a number of biomechanically responsive genes including KRT-6a/16, IL1RL1, and AQP3 among others.

Many of the different synergies represented as combinations of genes/proteins have been experimentally tested and published. However, there are combinations that have yet to be explored. I address the problem of identifying these unexplored combinations via use of a machine learning based search engine in the next section.

1.5. Insight Behind the Work

Across all search engines has the fundamental principle remains the same i.e to capture the pattern available in the data and based on that pattern, rank a list of queries. Different algorithms can be applied, however if the fundamental pattern is captured accurately, then the rankings will remain approximately the same, with slight variations, across the different kinds of search engines used. I use one search engine, however, vary the way the patterns are captured via use of different sensitivity methods. Each sensitivity method uses a different flavour/mathematical formulation to compute the sensitivity indices to estimate the influence of the involved factors. These involved factors are genes that play a role in cell biology, in the above research. The insight is that all methods will capture the sensitivity of the involved factors based on their recorded regulations and the search engine will rank the combination of factors based on these sensitivity indices. Since the role of involved factors are captured properly, the search engine will give appropriate rankings to the combinations, thus capturing which gene combinations might be playing significantly in a biological phenomena. The above work shows rankings for experimentally confirmed combinations as well as unexplored/untested combinations. These rankings are not just numbers. They point to the existence of biological synergy in the form of gene combinations, whether tested in wet lab or unexplored till now. Finally, the findings suggest that the rankings are conserved across the different sensitivity methods used.

1.6. Combinatorial Search Problem and a Possible Solution

In a recently published work [2], a frame work of a search engine was developed which can rank combinations of factors (genes/proteins) in a signaling pathway. The work uses SVM package by [28] in https://www.cs.cornell.edu/people/tj/svm_light/svm_rank.html. I use the adaptation to rank 2^{nd} order gene combinations. The sensitivity package by [29] was used to develop the search engine pipeline. The current research uses the Hilbert Schmidt Independence Criterion (HSIC) and SOBOL method, implemented in the sensitivity package mentioned above. I use three different kernels under the HSIC method namely, • laplace, • linear and • rbf. For SOBOL method, I use • sobol-2002, and • sobol-jansen. Each of these variants or kernels have been implemented in the sensitivity package and option has been provided in the search engine code to generate the rankings for a particular gene, using a choice of a kernel/variant at a time. Technical details about the variants and kernels can be found in references citetd in [29].

 doi:10.20944/preprints202505.1982.v1

2. Methods

2.1. Static Data from [1]

Patel et al. [1] analyzed 160 meningioma samples from 140 patients, and according to the WHO histopathological classification system for meningioma, they found 121 tumors were of grade I (benign), 32 were of grade II (atypical), and 7 were of grade III (malignant). To determine whether meningiomas could be differentiated based on gene expression profiles, they used principal component analysis (PCA) on a discovery set of 97 tumors (i.e 77 WHO grade I and 20 WHO grade II). Next, they employed nonnegative matrix factorization (NMF) clustering (a unsupervised machine-learning approach) for k = 2 to k = 7 using the 1,500 genes that varied most among the tumor samples. They report that after 1,000 iterations, 3 clusters (k = 3) emerged as providing the best fit as determined by the consensus membership, cophenetic, and silhouette scores. They evaluated the cluster significance of the 3 subtypes using SigClust (Huang et al. [30]) and observed statistical significance between cluster boundaries, which exhibited significant differences in WHO grade representation.

2.2. Design for Static Data from [1]

The procedure begins with the listing of all C_k^n combinations for k number of genes from a total of n genes. Here n can be the choice of the biologist. k is ≥ 2 and $\leq (n-1)$. Each of the combination of order k represent a unique set of interaction between the involved genetic factors. Since the sensitivity analysis methods require a sample for a particular observation, a steep gaussian distribution was generated with a jitter (noise) added to the deviation from the reported point measurement of 0.005. In this experiment, the distribution contained 10 measurements (including the point of measurement under consideration). This is repeated for each point of measurement.

To have an averaged ranking, the experiment was designed to run for 25 iterations. In each iteration, the datasets are combined in a specifed format which go as input as per the requirement of a particular sensitivity analysis method. Thus for each p^{th} combination in C_k^n combinations, the dataset is prepared in a required format. Details of formatting the data have not been presented in the article to maintain the fluidity and brevity. Interested readers can find examples of formating the data in the sensitivity analysis package in R. Sensitivity analysis and its relevance in systems biology have been covered in a recently published article by [31], which forms the foundation for this work. After the data has been transformed, vectorized programming is employed for density based sensitivity analysis and looping is employed for variance based sensitivity analysis to compute the required sensitivity indices for each of the p combinations.

After the above sensitivity indices have been stored for each of the p^{th} combination, for a chosen sensitivity analysis method, the next step in the design of experiment is conducted. Here, the indices are averaged per combination to have a mean index value. These index values form the discriminative features for a particular combination. For a k^{th} order combination, a vector of k elements or indices forms a feature vector. Thus for C_k^n combinations there will be C_k^n vectors, each containing k elements. Next, SVM_{learn}^{Rank} [28] is used to generate a model on default value C value of 20. In the current experiment on toy model C value has not been tunned. The training set helps in the generation of the model as the different gene combinations are numbered in order which are used as rank indices. The model is then used to generate score on the observations in the testing set using the $SVM_{classify}^{Rank}$ [28]. This is followed by sorting of these scores along with the rank indices already assigned to the gene combinations. The end result is a sorted order of the gene combinations based on the ranking score learned by the SVM^{Rank} algorithm.

Note that the following is the order in which the files should be executed in R [32], in order, for obtaining the desired results (Note that the code will not be explained here) - • use source("extractMeningiomadata.R") • use source("manuscript-2-2.R") • use source("SVMRank-Results-S-mean.R").

 doi:10.20944/preprints202505.1982.v1

2.3. Translating the Pipeline Into Code of Execution in R

The execution begins by some preprocessing of the file containing the information regarding the down regulated genes via $source(\text{“}extractMeningiomadata.R\text{”})$. The library containing the sensitivity analysis methods is then loaded in the interface using the command $library(sensitivity)$ (Note - this package can be downloaded for free from https://cran.r-project.org/web/packages/sensitivity/index.html). Next a gaussian distribution for a particular transcript level for a gene is generated to have a sample. This is needed in the computation of sensitivity index for that particular gene. A gene of particular choice is selected (in blue) and the choice of the combination is made (here k = 2). Later a kernel is used (here rbf for HSIC method). 25 different indices are generated which help in generating aggregate rank using these 25 indices. The Support vector ranking algorithm is employed to generate the scores for different combinations and these scores are then sorted out. This is done using the command $source(\text{”}SVMRank-Results-S-mean.R\text{”})$. A file is generated that contains the combinations in increasing order of influence. Note that 1 means lowest rank and vice versa, for 2^{nd} order combinations for any gene using a particular density based sensitivity index.

2.4. Regarding Biological Insight

For the recorded gene expression values, the sensitivity indices are computed. The search engine uses the kernel based density method. The kernel method takes the data, that is in a lower dimensional plane and projects it to a higher dimensional plane, with an idea that in a higher dimensional place, there exists a dot product between the projected data. To simply state, the idea is that in a higher dimensional plane the nonlinearities between the data (in lower dimensional plane) will be captured and the data may be segregated from each other via a hyperplane. So, irrespective of the method used to measure the gene expression values, if the measurements capture biological information (to whatever extent they can), then the kernel method will be able to capture the nonlinearities/synergies, if existing and allow the sensitivity analysis method (here density based method) to estimate the strength of influence of each of the factors. Based on the sensitivity indices of combinations of a particular order, the search engine ranks the combinations. Details of search engine are provided in the published work in [2].

It is important to note that the search engine will not give insight about the mechanism of synergy between the components of a combination. However, if the synergy exists between components of an unexplored/untested combination, then the sensitivity indices will capture the influence of these components taken together (which form a combination of interest) and will rank the combination appropriately. These rankings provide insight about which combination a biologist/oncologist might want to test in a forest of combinations for a given scenario in a cell (whether normal or pathalogical).

3. Results & Discussion

3.1. AQP3 Related Synergies

Note - AQP3 was found to be upregulated in Type A. Upregulation was defined as Type logFC to be > 1 and FDR ≤ 0.001, in Patel et al. [1]. Also, sorting of scores by the machine learning algorithm were donw in ascending order, i.e - top is lowest in ranking. A total of 307 2^{nd} order combinations of AQP3 were recorded.

3.1.1. AQP3—Individual Genes

The following genes were found to show high rankings along with AQP3 - USH1 protein network component harmonin (USH1C), mucolipin TRP cation channel 3 (MCOLN3), erb-b2 receptor tyrosine kinase 3 (ERBB3), galanin and GMAP prepropeptide (GAL), ST6 N-acetylgalactosaminide alpha-2,6-sialyltransferase 2 (ST6GALNAC2), calpain 6 (CAPN6), immunoglobulin superfamily member 9 (IGSF9), ATP binding cassette subfamily B member 1 (ABCB1), parathyroid hormone like hormone (PTHLH), PITPNM family member 3 (PITPNM3), tolloid like 2 (TLL2), neurotensin receptor 1 (NTSR1), mesothelin (MSLN), annexin A13 (ANXA13), Rap guanine nucleotide exchange factor like 1

 doi:10.20944/preprints202505.1982.v1

(RAPGEFL1), protein arginine methyltransferase 8 (PRMT8), interleukin 1 receptor like 1 (IL1RL1), interferon regulatory factor 6 (IRF6), phospholipid phosphatase related 4 (PLPPR4), cyclin and CBS domain divalent metal cation transport mediator 1 (CNNM1), proprotein convertase subtilisin/kexin type 2 (PCSK2), kallikrein related peptidase 8 (KLK8), proline rich and Gla domain 3 (PRRG3), BICD family like cargo adaptor 1 (BICDL1), FXYD domain containing ion transport regulator 6 (FXYD6), epidermal growth factor (EGF), maelstrom spermatogenic transposon silencer (MAEL), immunoglobulin like domain containing receptor 2 (ILDR2), sushi domain containing 4 (SUSD4), glutamate decarboxylase like 1 (GADL1), solute carrier family 26 member 7 (SLC26A7), C3 and PZP like alpha-2-macroglobulin domain containing 8 (CPAMD8), cytochrome c oxidase subunit 6B2 (COX6B2), sphingosine-1-phosphate phosphatase 2 (SGPP2), gamma-aminobutyric acid type A receptor subunit gamma1 (GABRG1), neuropeptide Y receptor Y1 (NPY1R), hyperpolarization activated cyclic nucleotide gated potassium channel 1 (HCN1), defensin beta 1 (DEFB1), WNK lysine deficient protein kinase 2 (WNK2), phytanoyl-CoA 2-hydroxylase interacting protein like (PHYHIPL), solute carrier family 16 member 9 (SLC16A9), protein phosphatase 1 regulatory subunit 36 (PPP1R36), calcium voltage-gated channel auxiliary subunit beta 2 (CACNB2), serine peptidase inhibitor, Kunitz type 1 (SPINT1), sodium voltage-gated channel beta subunit 3 (SCN3B), ubiquitin specific peptidase 54 (USP54), serpin family B member 8 (SERPINB8), coiled-coil domain containing 68 (CCDC68), pleckstrin homology domain containing A7 (PLEKHA7), alanyl aminopeptidase, membrane (ANPEP), myosin IA (MYO1A), small G protein signaling modulator 1 (SGSM1), glycerol-3-phosphate dehydrogenase 1 (GPD1), dynein axonemal assembly factor 3 (DNAAF3), phospholipase A and acyltransferase 5 (HRASLS5), bradykinin receptor B2 (BDKRB2), phytanoyl-CoA 2-hydroxylase interacting protein (PHYHIP), neuronal vesicle trafficking associated 1 (NSG1), proprotein convertase subtilisin/kexin type 9 (PCSK9), RAB3B, member RAS oncogene family (RAB3B), mucin 3A, cell surface associated (MUC3A), OTU deubiquitinase 7A (OTUD7A), DLG associated protein 1 (DLGAP1), heparan sulfate 6-O-sulfotransferase 2 (HS6ST2), CDC42 binding protein kinase gamma (CDC42BPG), potassium two pore domain channel subfamily K member 3 (KCNK3), lysophosphatidic acid receptor 3 (LPAR3), anoctamin 5 (ANO5), cilia and flagella associated protein 46 (CFAP46), angiopoietin like 7 (ANGPTL7), interferon stimulated exonuclease gene 20 (ISG20), membrane bound glycerophospholipid O-acyltransferase 1 (MBOAT1), tryptase alpha/beta 1 (TPSAB1), serine palmitoyltransferase long chain base subunit 3 (SPTLC3), bisphosphoglycerate mutase (BPGM), cold shock domain containing C2 (CSDC2), regulator of calcineurin 2 (RCAN2), radial spoke head component 9 (RSPH9), carboxylesterase 4A (CES4A), ciliary microtubule associated protein 3 (CIMAP3 / PIFO), leucine rich repeat and Ig domain containing 2 (LINGO2), solute carrier organic anion transporter family member 2A1 (SLCO2A1), solute carrier family 35 member G1 (SLC35G1), myosin ID (MYO1D), family with sequence similarity 91 member A1 (FAM91A1), potassium voltage-gated channel subfamily A member 2 (KCNA2), LRRN4 C-terminal like (LRRN4CL), G protein-coupled receptor 4 (GPR4), reprimo, TP53 dependent G2 arrest mediator homolog (RPRM), endoplasmic reticulum to nucleus signaling 1 (ERN1), transmembrane protein 125 (TMEM125), WSC domain containing 1 (WSCD1), transmembrane protein 30B (TMEM30B), synemin (SYNM), calpain 12 (CAPN12), receptor interacting serine/threonine kinase 4 (RIPK4), family with sequence similarity 162 member B (FAM162B), aldehyde dehydrogenase 1 family member A3 (ALDH1A3), coiled-coil serine rich protein 1 (CCSER1), brain expressed X-linked 5 (BEX5), oxysterol binding protein 2 (OSBP2), short chain dehydrogenase/reductase family 42E, member 1 (SDR42E1), MAF bZIP transcription factor F (MAFF), RNA binding motif protein 11 (RBM11), transcobalamin 2 (TCN2), limbic system associated membrane protein (LSAMP), piccolo presynaptic cytomatrix protein (PCLO), insulin induced gene 1 (INSIG1), NF2, moesin-ezrin-radixin like (MERLIN) tumor suppressor (NF2), BCR activator of RhoGEF and GTPase (BCR), metallophosphoesterase domain containing 1 (MPPED1), forkhead box I2 (FOXI2), keratin 16 (KRT16), natural killer cell cytotoxicity receptor 3 ligand 1 (NCR3LG1), phospholipase A2 group IIA (PLA2G2A), family with sequence similarity 78 member B (FAM78B), FAT atypical cadherin 4 (FAT4), solute carrier family 6 member 9 (SLC6A9), laminin subunit beta 3 (LAMB3), tryptase beta 2 (TPSB2), ectonucleotide pyrophosphatase/phosphodiesterase 1 (ENPP1), AFDN divergent transcript

 doi:10.20944/preprints202505.1982.v1

(AFDN-DT), DDB1 and CUL4 associated factor 12 like 2 (DCAF12L2), SH3 domain binding glutamate rich protein like 2 (SH3BGRL2), ankyrin repeat domain 35 (ANKRD35), sterol regulatory element binding transcription factor 2 (SREBF2), collagen type XV alpha 1 chain (COL15A1), family with sequence similarity 120A2, pseudogene (C9orf129) and SEC14 like lipid binding 6 (SEC14L6).

Using the adaptation of the above mentioned search engine, I was able to tabulate 2^{nd} order combinations of AQP3 with these genes, that were reported to be upregulated in [1].

Table 1 and 2 shows rankings of these combinations. Followed by this is the unexplored combinatorial hypotheses in Table 3 generated from analysis of the ranks in Table 1 and 2.

Table 1. 2^{nd} order interaction ranking between AQP3 VS Individual members.

Ranking Individual members VS AQP3								
	Ranking of Individual members w.r.t AQP3							
	laplace	linear	rbf	jansen		laplace	linear	rbf	jansen
USH1C - AQP3	245	205	200	15	MCOLN3 - AQP3	235	194	202	1
ERBB3 - AQP3	189	191	168	19	GAL - AQP3	180	161	134	161
ST6GALNAC2 - AQP3	177	163	158	63	CAPN6 - AQP3	201	177	148	34
IGSF9 - AQP3	49	154	137	156	ABCB1 - AQP3	249	176	187	45
PTHLH - AQP3	155	174	227	38	PITPNM3 - AQP3	148	178	201	174
TLL2 - AQP3	204	175	189	62	NTSR1 - AQP3	194	200	205	12
MSLN - AQP3	227	202	203	14	ANXA13 - AQP3	221	167	157	149
RAPGEFL1 - AQP3	173	72	149	189	PRMT8 - AQP3	184	193	173	59
IL1RL1 - AQP3	176	170	164	10	IRF6 - AQP3	198	148	169	126
PLPPR4 - AQP3	214	189	197	29	CNNM1 - AQP3	219	100	144	218
PCSK2 - AQP3	212	201	209	2	KLK8 - AQP3	242	206	198	26
PRRG3 - AQP3	163	190	165	6	BICDL1 - AQP3	196	197	170	68
FXYD6 - AQP3	164	160	208	49	EGF - AQP3	168	88	163	184
MAEL - AQP3	208	203	235	135	ILDR2 - AQP3	255	243	210	81
SUSD4 - AQP3	188	183	190	17	GADL1 - AQP3	203	192	154	28
SLC26A7 - AQP3	236	220	242	85	CPAMD8 - AQP3	152	142	69	152
COX6B2 - AQP3	161	210	185	13	SGPP2 - AQP3	207	180	138	61
GABRG1 - AQP3	202	165	250	9	NPY1R - AQP3	145	173	177	77
HCN1 - AQP3	232	214	152	67	DEFB1 - AQP3	266	276	221	47
WNK2 - AQP3	256	179	229	51	PHYHIPL - AQP3	273	256	260	229
SLC16A9 - AQP3	182	248	222	129	PPP1R36 - AQP3	265	265	248	141
CACNB2 - AQP3	226	299	289	148	SPINT1 - AQP3	303	273	278	132
SCN3B - AQP3	248	240	274	158	USP54 - AQP3	283	267	301	230
SERPINB8 - AQP3	286	307	286	296	CCDC68 - AQP3	222	215	186	40
PLEKHA7 - AQP3	274	264	297	274	ANPEP - AQP3	263	249	287	133
MYO1A - AQP3	247	209	257	114	SGSM1 - AQP3	297	304	293	232
GPD1 - AQP3	190	287	194	136	DNAAF3 - AQP3	251	241	249	159
HRASLS5 - AQP3	227	222	217	37	BDKRB2 - AQP3	233	232	232	24
PHYHIP - AQP3	199	212	243	32	NSG1 - AQP3	254	279	262	162
PCSK9 - AQP3	224	223	228	27	RAB3B - AQP3	239	251	245	137
MUC3A - AQP3	191	207	223	11	OTUD7A - AQP3	261	298	267	255
DLGAP1 - AQP3	268	271	211	131	HS6ST2 - AQP3	179	219	214	22

 doi:10.20944/preprints202505.1982.v1

Table 2. 2^{nd} order interaction ranking between AQP3 VS Individual members.

Ranking Individual members VS AQP3									
	Ranking of Individual members w.r.t AQP3								
	laplace	linear	rbf	jansen		laplace	linear	rbf	jansen
CDC42BPG - AQP3	305	226	285	213	KCNK3 - AQP3	223	235	226	36
LPAR3 - AQP3	238	216	236	70	ANO5 - AQP3	244	258	263	78
CFAP46 - AQP3	279	270	281	278	ANGPTL7 - AQP3	299	233	280	263
ISG20 - AQP3	302	269	276	172	MBOAT1 - AQP3	294	229	305	270
TPSAB1 - AQP3	170	246	246	58	SPTLC3 - AQP3	272	277	303	287
BPGM - AQP3	267	268	300	206	CSDC2 - AQP3	230	259	247	44
RCAN2 - AQP3	288	263	302	226	RSPH9 - AQP3	253	261	265	199
CES4A - AQP3	271	274	288	201	PIFO - AQP3	282	296	290	195
LINGO2 - AQP3	187	260	234	130	SLCO2A1 - AQP3	262	244	283	209
SLC35G1 - AQP3	277	282	396	256	MYO1D - AQP3	220	234	266	75
FAM91A1 - AQP3	301	306	271	252	KCNA2 - AQP3	269	247	292	125
LRRN4CL - AQP3	285	278	255	279	GPR4 - AQP3	264	288	298	264
RPRM - AQP3	195	218	179	52	ERN1 - AQP3	287	257	307	234
TMEM125 - AQP3	241	286	270	171	WSCD1 - AQP3	281	275	295	275
SYNM - AQP3	260	290	240	116	CAPN12 - AQP3	304	245	296	186
RIPK4 - AQP3	240	213	237	56	FAM162B - AQP3	231	237	239	87
ALDH1A3 - AQP3	216	227	224	80	CCSER1 - AQP3	289	228	219	185
BEX5 - AQP3	292	255	218	74	OSBP2 - AQP3	259	293	241	120
SDR42E1 - AQP3	211	231	277	124	MAFF - AQP3	280	280	258	222
RBM11 - AQP3	278	285	238	233	TCN2 - AQP3	284	305	304	258
LSAMP - AQP3	229	292	216	110	PCLO - AQP3	215	238	233	41
INSIG1 - AQP3	307	297	284	306	NF2 - AQP3	275	291	264	181
BCR - AQP3	246	302	268	257	MPPED1 - AQP3	209	224	213	3
FOXI2 - AQP3	186	252	225	4	KRT16 - AQP3	228	230	231	35
NCR3LG1 - AQP3	290	266	261	246	PLA2G2A - AQP3	141	239	199	5
FAM78B - AQP3	250	262	299	219	FAT4 - AQP3	234	236	256	98
SLC6A9 - AQP3	298	284	259	154	LAMB3 - AQP3	293	281	279	109
TPSB2 - AQP3	276	217	252	99	ENPP1 - AQP3	291	295	251	153
AFDN-DT - AQP3	296	303	291	280	DCAF12L2 - AQP3	185	204	206	21
SH3BGRL2 - AQP3	306	253	275	140	ANKRD35 - AQP3	300	301	282	281
SREBF2 - AQP3	270	289	294	282	COL15A1 - AQP3	295	283	269	238
C9orf129 - AQP3	252	272	273	96	SEC14L6 - AQP3	237	294	244	107

One can also interpret the results of the table 1 and 2 graphically, with the following influences - • Individual members w.r.t AQP3 with AQP3 $-$ > USH1C / MCOLN3 / ERBB3 / GAL / ST6GALNAC2 / CAPN6 / IGSF9 / ABCB1 / PTHLH / PITPNM3 / TLL2 / NTSR1 / MSLN / ANXA13 / RAPGEFL1 / PRMT8 / IL1RL1 / IRF6 / PLPPR4 / CNNM1 / PCSK2 / KLK8 / PRRG3 / BICDL1 / FXYD6 / EGF / MAEL / ILDR2 / SUSD4 / GADL1 / SLC26A7 / CPAMD8 / COX6B2 / SGPP2 / GABRG1 / NPY1R / HCN1 / DEFB1 / WNK2 / PHYHIPL / SLC16A9 / PPP1R36 / CACNB2 /SPINT1 / SCN3B / USP54 / SERPINB8 / CCDC68 / PLEKHA7 / ANPEP / MYO1A / SGSM1 / GPD1 / DNAAF3 / HRASLS5 / BDKRB2 / PHYHIP / NSG1 / PCSK9 / RAB3B / MUC3A / OTUD7A / DLGAP1 /

 doi:10.20944/preprints202505.1982.v1

HS6ST2 / CDC42BPG / KCNK3 / LPAR3 / ANO5 / CFAP46 / ANGPTL7 / ISG20 / MBOAT1 / TPSAB1 / SPTLC3 / BPGM / CSDC2 / RCAN2 / RSPH9 / CES4A / PIFO / LINGO2 / SLCO2A1 / SLC35G1 / MYO1D / FAM91A1 / KCNA2 / LRRN4CL / GPR4 / RPRM / ERN1 / TMEM125 / WSCD1 / SYNM / CAPN12 / RIPK4 / FAM162B / ALDH1A3 / CCSER1 / BEX5 / OSBP2 / SDR42E1 / MAFF / RBM11 / TCN2 / LSAMP / PCLO / INSIG1 / NF2 / BCR / MPPED1 / FOXI2 / KRT16 / NCR3LG1 / PLA2G2A / FAM78B / FAT4 / SLC6A9 / LAMB3 / TPSB2 / ENPP1 / AFDN-DT / DCAF12L2 / SH3BGRL2 / ANKRD35 / SREBF2 / COL15A1 / C9orf129 / SEC14L6.

Table 3. 2^{nd} order combinatorial hypotheses between AQP3 and Individual members.

UNEXPLORED COMBINATORIAL HYPOTHESES	
Individual members w.r.t AQP3	
USH1C / MCOLN3 / ERBB3 / GAL / ST6GALNAC2...	
CAPN6 / IGSF9 / ABCB1 / PTHLH / PITPNM3...	
TLL2 / NTSR1 / MSLN / ANXA13 / RAPGEFL1...	
PRMT8 / IL1RL1 / IRF6 / PLPPR4 / CNNM1...	
PCSK2 / KLK8 / PRRG3 / BICDL1 / FXYD6...	
EGF / MAEL / ILDR2 / SUSD4 / GADL1...	
SLC26A7 / CPAMD8 / COX6B2 / SGPP2 / GABRG1...	
NPY1R / HCN1 / DEFB1 / WNK2 / PHYHIPL...	
SLC16A9 / PPP1R36 / CACNB2 /SPINT1...	
SCN3B / USP54 / SERPINB8 / CCDC68 / PLEKHA7...	
ANPEP / MYO1A / SGSM1 / GPD1 / DNAAF3...	
HRASLS5 / BDKRB2 / PHYHIP / NSG1 / PCSK9...	
RAB3B / MUC3A / OTUD7A / DLGAP1 / HS6ST2...	
CDC42BPG / KCNK3 / LPAR3 / ANO5 / CFAP46...	
ANGPTL7 / ISG20 / MBOAT1 / TPSAB1 / SPTLC3...	
BPGM / CSDC2 / RCAN2 / RSPH9 / CES4A / PIFO...	
LINGO2 / SLCO2A1 / SLC35G1 / MYO1D / FAM91A1...	
KCNA2 / LRRN4CL / GPR4 / RPRM / ERN1 / TMEM125...	
WSCD1 / SYNM / CAPN12 / RIPK4 / FAM162B...	
ALDH1A3 / CCSER1 / BEX5 / OSBP2 / SDR42E1...	
MAFF / RBM11 / TCN2 / LSAMP / PCLO / INSIG1...	
NF2 / BCR / MPPED1 / FOXI2 / KRT16 / NCR3LG1...	
PLA2G2A / FAM78B / FAT4 / SLC6A9 / LAMB3 / TPSB2...	
ENPP1 / AFDN-DT / DCAF12L2 / SH3BGRL2 / ANKRD35...	
SREBF2 / COL15A1 / C9orf129 / SEC14L6	AQP3

4. Conclusions

Presented here are a range of multiple synergistic AQP3 2^{nd} order combinations that were ranked via a machine learning based search engine. Via majority voting across the ranking methods, it was possible to find plausible unexplored synergistic combinations of AQP3-X that might be prevalent in meningioma.

Author Contributions: Concept, design, in silico implementation - SS. Analysis and interpretation of results - SS. Manuscript writing - SS. Manuscript revision - SS. Approval of manuscript - SS.

Data Availability Statement: Data used in this research work was released in a publication in Patel et al. [1]. Permission to use, granted by PNAS.

 doi:10.20944/preprints202505.1982.v1

Acknowledgments: Special thanks to Mrs. Rita Sinha and Mr. Prabhat Sinha for supporting the author financially, without which this work could not have been made possible.

Conflicts of Interest: There are no conflicts to declare.

References

1. Patel, A.J.; Wan, Y.W.; Al-Ouran, R.; Revelli, J.P.; Cardenas, M.F.; Oneissi, M.; Xi, L.; Jalali, A.; Magnotti, J.F.; Muzny, D.M.; et al. Molecular profiling predicts meningioma recurrence and reveals loss of DREAM complex repression in aggressive tumors. *Proceedings of the National Academy of Sciences* **2019**, *116*, 21715–21726.
2. Sinha, S. Machine learning ranking of plausible (un) explored synergistic gene combinations using sensitivity indices of time series measurements of Wnt signaling pathway. *Integrative Biology* **2024**, *16*, zyae020.
3. Louis, D.N.; Perry, A.; Wesseling, P.; Brat, D.J.; Cree, I.A.; Figarella-Branger, D.; Hawkins, C.; Ng, H.; Pfister, S.M.; Reifenberger, G.; et al. The 2021 WHO classification of tumors of the central nervous system: a summary. *Neuro-oncology* **2021**, *23*, 1231–1251.
4. Torp, S.H.; Solheim, O.; Skjulsvik, A.J. The WHO 2021 Classification of Central Nervous System tumours: a practical update on what neurosurgeons need to know—a minireview. *Acta Neurochirurgica* **2022**, *164*, 2453–2464.
5. Czarnetzki, A.; Schwaderer, E.; Pusch, C.M. Fossil record of meningioma. *The Lancet* **2003**, *362*, 408.
6. Okonkwo, D.O.; Laws Jr, E.R. Meningiomas: historical perspective. In *Meningiomas*; Springer, 2009; pp. 3–10.
7. Paterniti, S. Meningiomas surgery in Italy in the nineteenth century: Historical review. *Austin Neurosurg Open Access* **2015**, *2*, 1030.
8. Pecchioli, Z. Soria di un fungo della dura madre, operato coll'estirpazione dal Professor Zanobi Pecchioli. *Nuovo Giornale de'Letterati—Scienze* **1838**, *36*, 39–44.
9. Cushing, H. The meningiomas (dural endotheliomas): their source, and favoured seats of origin. *Brain* **1922**, *45*, 282–316.
10. contributors, W. Meningioma — Wikipedia, The Free Encyclopedia, 2024. Online; accessed 11-April-2025.
11. Pamir, M.N.; Black, P.M.; Fahlbusch, R. *Meningiomas : a comprehensive text*; Elsevier Health Sciences, 2010.
12. Szulzewsky, F.; Thirimanne, H.N.; Holland, E.C. Meningioma: current updates on genetics, classification, and mouse modeling. *Upsala Journal of Medical Sciences* **2024**, *129*, 10–48101.
13. Verkman, A.; Mitra, A.K. Structure and function of aquaporin water channels. *American Journal of Physiology-Renal Physiology* **2000**, *278*, F13–F28.
14. Benga, G.; Popescu, O.; Pop, V.I.; Holmes, R.P. p-(Chloromercuri) benzenesulfonate binding by membrane proteins and the inhibition of water transport in human erythrocytes. *Biochemistry* **1986**, *25*, 1535–1538.
15. Denker, B.M.; Smith, B.L.; Kuhajda, F.P.; Agre, P. Identification, purification, and partial characterization of a novel Mr 28,000 integral membrane protein from erythrocytes and renal tubules. *Journal of biological chemistry* **1988**, *263*, 15634–15642.
16. Preston, G.M.; Carroll, T.P.; Guggino, W.B.; Agre, P. Appearance of water channels in Xenopus oocytes expressing red cell CHIP28 protein. *Science* **1992**, *256*, 385–387.
17. Agre, P.; Preston, G.M.; Smith, B.L.; Jung, J.S.; Raina, S.; Moon, C.; Guggino, W.B.; Nielsen, S. Aquaporin CHIP: the archetypal molecular water channel. *American Journal of Physiology-Renal Physiology* **1993**, *265*, F463–F476.
18. Benga, G. Birth of water channel proteins—the aquaporins. *Cell Biology International* **2003**, *27*, 701–709.
19. Knepper, M.A.; Nielsen, S. Peter Agre, 2003 Nobel Prize winner in chemistry. *Journal of the American Society of Nephrology* **2004**, *15*, 1093–1095.
20. Kuchel, P. The story of the discovery of aquaporins: convergent evolution of ideas—but who got there first. *Cell Mol Biol (Noisy-le-grand)* **2006**, *52*, 2–5.
21. Ishibashi, K.; Sasaki, S.; Fushimi, K.; Uchida, S.; Kuwahara, M.; Saito, H.; Furukawa, T.; Nakajima, K.; Yamaguchi, Y.; Gojobori, T. Molecular cloning and expression of a member of the aquaporin family with permeability to glycerol and urea in addition to water expressed at the basolateral membrane of kidney collecting duct cells. *Proceedings of the National Academy of Sciences* **1994**, *91*, 6269–6273.
22. Ishibashi, K.; Sasaki, S.; Saito, F.; Ikeuchi, T.; Marumo, F. Structure and chromosomal localization of a human water channel (AQP3) gene. *Genomics* **1995**, *27*, 352–354.
23. Inase, N.; Fushimi, K.; Ishibashi, K.; Uchida, S.; Ichioka, M.; Sasaki, S.; Marumo, F. Isolation of human aquaporin 3 gene. *Journal of Biological Chemistry* **1995**, *270*, 17913–17916.

 doi:10.20944/preprints202505.1982.v1

24. Mulders, S.; Olde Weghuis, D.; Van Boxtel, J.; Geurts van Kessel, A.; Echevarria, M.; Van Os, C.; Deen, P. Localization of the human gene for aquaporin 3 (AQP3) to chromosome 9, region p21→ p12, using fluorescent in situ hybridization. *Cytogenetic and Genome Research* **1996**, *72*, 303–305.
25. Ma, T.; Song, Y.; Yang, B.; Gillespie, A.; Carlson, E.J.; Epstein, C.J.; Verkman, A. Nephrogenic diabetes insipidus in mice lacking aquaporin-3 water channels. *Proceedings of the National Academy of Sciences* **2000**, *97*, 4386–4391.
26. Roudier, N.; Ripoche, P.; Gane, P.; Le Pennec, P.Y.; Daniels, G.; Cartron, J.P.; Bailly, P. AQP3 deficiency in humans and the molecular basis of a novel blood group system, GIL. *Journal of Biological Chemistry* **2002**, *277*, 45854–45859.
27. Tsitsikov, E.N.; Hameed, S.; Tavakol, S.A.; Stephens, T.M.; Tsytsykova, A.V.; Garman, L.; Bi, W.L.; Dunn, I.F. Specific gene expression signatures of low grade meningiomas. *Frontiers in Oncology* **2023**, *13*, 1126550.
28. Joachims, T. Training linear SVMs in linear time. In Proceedings of the Proceedings of the 12th ACM SIGKDD international conference on Knowledge discovery and data mining. ACM, 2006, pp. 217–226.
29. Pujol, G.; Iooss, B.; Janon, A.; Boumhaout, K.; Da Veiga, S.; Fruth, J.; Gilquin, L.; Guillaume, J.; Le Gratiet, L.; Lemaitre, P.; et al. Sensitivity: global sensitivity analysis of model outputs. *R package version* **2017**, *1*.
30. Huang, H.; Liu, Y.; Yuan, M.; Marron, J. Statistical significance of clustering using soft thresholding. *Journal of Computational and Graphical Statistics* **2015**, *24*, 975–993.
31. Sinha, S. Hilbert-Schmidt and Sobol sensitivity indices for static and time series Wnt signaling measurements in colorectal cancer-part A. *BMC systems biology* **2017**, *11*, 120.
32. Team, R.C. R language definition. *Vienna, Austria: R foundation for statistical computing* **2000**, *3*, 116.